Polysaccharide-induced apoptosis in H22 cells through G2/M arrest and BCL2/BAX caspase-activated Fas pathway

W. Song[1, 2✉], C. Song[1, 2*], Y. Chen[3*], M. Du[1, 2], P. Hu[4], A. Liu[5] and W. Lu[1,2✉]

[1] Institute of Extreme Environment Nutrition and Protection, Harbin Institute of Technology, Harbin 150090, China
[2] Department of Food Science and Engineering, Harbin Institute of Technology, Harbin 150090, China
[3] Gaoping, Shanxi, 048400, China
[4] Department of Life Science, Lvliang University, Lvliang 033001, China
[5] Key Laboratory of Food Nutrition and Safety, Ministry of Education, Tianjin University of Science and Technology, Tianjin 300457, China

Corresponding author: Wei Song, Institute of Extreme Environment Nutrition and Protection; Department of Food Science and Engineering, Harbin Institute of Technology, Harbin 150090, China. Email: weisong@hit.edu.cn and Weihong Lu, Institute of Extreme Environment Nutrition and Protection; Department of Food Science and Engineering, Harbin Institute of Technology, Harbin 150090, China. Email: lwh@hit.edu.cn
* The authors contribute equally to this work.

Abstract

The aim of the present work was to investigate the effect and the mechanism of growth inhibition on mouse H22 hepatocarcinoma cell of ascitic tumor induced by cartilage polysaccharides (PS). Our results showed that PS prolonged the survival time of the mice and increased the life span. In addition, PS induced the apoptosis of the H22 cells with the typical apoptotic morphological and biochemical changes confirmed by HE staining and TUNEL assay. The subsequent analysis of cell cycle distribution and relevant proteins revealed that decrease of cells in G0/G1phase and a G2/M arrest might due to the down-regulation of Cyclin D1 and AFP and up-regulation of P21 proteins. Moreover, BCL2/BAX caspase-activated Fas pathway was activated in PS-induced H22 apoptosis.

Key words: Cartilage polysaccharide, H22 hepatocarcinoma cell, Apoptosis, Cycle cell arrest, Fas.

Introduction

Liver cancer is one of the most common malignant tumor in China with a high mortality ratio after gastric and esophageal carcinoma (1). Tumorigenesis and tumor progression are associated not only with tumor cell proliferation, but also with cell apoptosis (2, 3). Recently, the induction of cell apoptosis is used as a target for the development of successful anti-carcinogens (4). The concept of apoptosis was introduced in 1972 by Kerr *et al* (5) and the typical apoptotic morphology was subsequently described in more details by Wyllie *et al* in 1980 (6). Apoptosis is a programmed cell death occurring under certain physiological or pathological conditions, which is necessary for the regulation of growth during development and to maintain an equilibrium in the physiological processes of multicellular organisms (7). As a programmed cell death, apoptosis undergo complicated and strictly regulated events associated with massive genes and proteins signaling pathway (8).

Extracellular death signal can be transferred into the cell through death receptors that are represented by a set of transmembrane proteins belonging to the tumor necrosis factor receptors (TNFR) gene superfamily (9). Death receptors bind with their corresponding ligands to transduce the apoptotic signals and induce the activation of caspases which exist as inactive proenzymes that undergo proteolytic processing at conserved aspartic residues to produce two subunits, large and small, that dimerize to form the active enzyme (10). Sequential activation of caspases plays a central role in the execution phase of cell apoptosis, triggering to the activation of caspase-3 that represent the last and final step of the cascade activation leading to cell apoptosis (11). Under certain circumstance, the above mentioned apoptotic pathway might be inhibited by BCL2 (B-cell lymphoma 2), encoded in humans by the *BCL2* gene (12-14). The BCL2 family proteins regulate apoptotic cell death by either inducing it (pro-apoptotic) or inhibiting it (anti-apoptotic). BCL2 is specifically considered as an important anti-apoptotic protein and is thus classified as an oncogene (15). BAX protein, another member of the BCL2 family encoded in humans by the *BAX* gene, promote apoptosis by binding and antagonizing the BCL2 protein (16). Besides apoptotic-associated proteins, Cyclin-dependent kinase (CDKs), such as Cyclin D1, also regulates the cell cycle to modulate cell proliferation or apoptosis (16, 17). Cyclin-dependent kinase inhibitor (CKI) is a negative regulatory factor that inhibits CDKs activity (18). P21, one of the major genes belonging to the CKI family, on one hand can combines with Cyclins, CDK and PCNA to form a tetramer compound to suppress Cyclin-CDK activity and to arrest the progress from G_1 to S phase, and on the other hand, can make a complex with PCNA sigma subunit of DNA polymerase to prevent DNA duplication (19, 20).

Polysaccharides possess multiple bioactivities including anti-tumor, anti-infection, immunity promotion, anti-rheumatic and anti-peptic ulcer (21). Several researches were focusing their attention on the antitumor activity of plant and fungi polysaccharides, such as panaxan, ganoderan and aloe polysaccharide (22-24). In recent years much attention has been paid to the effects of polysaccharides from animal sources against cancer.

Several studies showed that shark cartilage possesses angiogenic inhibitory effects and anti-tumor activities (25, 26). Our group showed that cartilage polysaccharide (PS) extracted and purified from porcine cartilage possessed a significant ability to inhibit S180 and MCF-7 cell proliferation (27). Based on our previous results, we performed an *in vivo* study on mice using the ascite H22 hepatocarcinoma cell line to investigate the anti-tumor effect of PS on H22 cell.

Materials and methods

Extraction of polysaccharide from porcine cartilage

Porcine cartilage was crushed with a colloid mill of 100 meshes, kept in HCl (0.1%) for 2 hours to remove the residual calcium salt, and washed with water until the sample reached a neutral pH. Next, 1% Na_2CO_3 was added and the temperature was kept at 70°C for 30 min. The product was hydrolyzed by papain (1:500, w/v) for 3 h, adsorbed by EDTA and eluted by NaCl, to extract the long chain polysaccharide. Finally, the long chain polysaccharide underwent degradation to obtain a short chain polysaccharide (PS) by H_2O_2 (3%) for 3 hours, followed by ethanol precipitation. And it was dried at room temperature. After lyophilization, PS was dissolved in Phosphate Buffer Solution (PBS) pH 7.4 for the *in vivo* study. PS at a concentration of 0.4 mg/mL was used to determine the purity of the samples with the HPLC system as described in our previous study. The PS from the porcine cartilage exhibited 95% chondroitin sulfate purity according to calculations based on the internal standard method (28). Moreover, in our previous study, one hundred micrograms of sample was run on a poly-acrylamide gel in parallel. Alcian blue staining showed that the average molecular weight of the sample was approximately 30 kDa. Protein staining by Coomassie blue R-250 demonstrated that the sample was pure (29).

Cell lines and materials

H22 cells (Tianjin Medical University, Tianjin, China) were cultured in RPMI 1640 (Thermo Scientific Hyclone, Shanghai, China) containing 10% heat-inactivated fetal bovine serum (Thermo Scientific Hyclone, Shanghai, China), 100 U/ml penicillin G, 100 µg/mL streptomycin (Gibco, Burlington, ON, Canada), and 2 mmol/L glutamine. KM mice (SPF) with a controlled weight of 26~28g were provided by the Department of Experimental Animals, Academy of Military Medical Sciences, Beijing. Same number of males and females mice was used. Five experimental groups were set for 1, 3 and 5 d PS treatment groups, vehicle control, and control group with PBS treatment. In each group there were 15 mice. The certification number was SCXK-(Military) 2002-001. All the animal experimental procedures followed The National Institutes of Health guidelines for the care and use of laboratory animals. The animals were allowed free access to food and water during the experiment and were maintained on a 12 h light/dark cycle in a controlled temperature (20-25°C) and humidity (50±5%) environment for 1 week before use.

Establishment of H22 cell-bearing mouse model

H22 cells were cultured in RPMI 1640 medium, ex-ponential phase cells were collected and washed with 0.9% saline for 3 times to adjusted to $1×10^7$/mL. One mL of H22 cell suspension was then intraperitoneally injected in KM mice. After 7 days ascites were absorbed collected and washed and the concentration was adjusted to $1×10^7$/mL with normal saline. This cell suspension was intraperitoneally injected in 20 KM mice at a dose of 0.2 mL/mouse on day 0. The next day, the mice were randomly divided into four groups: vehicle control and 1, 3 and 5d PS treated groups. The vehicle control was treated intraperitoneally with normal saline, whereas PS group was treated with 1500mg/kg PS per day. The average survival time of each group was recorded and the increase in life span (ILS) was calculated. ILS (%) = [(average lifespan in an experimental group − average life span in the vehicle control)/average life span in control group] × 100, where the experimental group is the PS group and the vehicle control is the group treated with normal saline. The organ index of thymus and spleen was calculated. Thymus index = thymus weight (mg)/body weight (g); Spleen index = spleen weight (mg)/body weight (g).

Apoptosis detection by HE staining

After PS treatment for 0, 1, 3 and 5d, the mice were sacrificed and sterilized with 75% ethanol. The ascites were then extracted from each mouse and washed with PBS (pH 7.3) two times. The discontinued density gradient centrifugation was used to separate the H22 cells. Briefly, 15 mL of 100% lymphocyte separating medium was added into the underlayer and 15 mL of 75% lymphocyte separating medium was added into the middle layer. A portion of 20 mL cell suspension was added into the centrifuge tube. The cells were collected at the 75% interface after centrifugation of 2000 rpm/min with 20 min. Erythrocyte lysis buffer was added and mixed well to stand for 8 min in the refrigerator at 4 °C. The mixture was then centrifuged for 5 min at 1500 rpm/min, the cells were washed with PBS and RPMI 1640 medium and fixed. The fixed cells were immersed in hematoxylin for 10 min and then washed with distilled water. Next, the cells were immersed in eosin for 3 min and washed with ethanol at different percentages. Cell morphology was analyzed by microscopy (Olympus, C5060-ADU, Tokyo, Japan).

Apoptosis detection by TUNEL staining

TUNEL assay is a staining specific for apoptotic cell nucleus or apoptotic bodies, therefore it allows to detect the typical morphology of apoptosis thanks to its ability to detect DNA fragmentation by labeling the terminal end of nucleic acids (28). In this study, an in situ apoptosis detection kit (Promega, Madison, WI, USA) was used to determine the induction of H22 apoptosis by PS treatment according to the manufacturer's protocol. Briefly, ascites were extracted (as describe in section 2.4) and washed with PBS, the cell suspension was pipetted onto the slides at a concentration of $1×10^6$/mL for 10 min. Fifty (50) µL of ice-cold rTdT incubation buffer was added to the cells and the slides were covered and incubated at 37 °C for 60 min in a humid chamber. Next, 2×SSC was used to immerse the slides in a Coplin jar for 15 min at room temperature to complete the reaction. The slides were then washed with fresh PBS

Table 1. Effect of PS on the survival time, increase in life span (ILF) and organ index.

Group	n	Survival time (d)	ILF (%)	Spleen index (mg/g)	Thymus index (mg/g)
Control	10	12.13±0.23	----	3.04±0.37	1.25±0.21
PS (1500mg/kg)	10	16.88±0.72*	38.56*	4.07±0.81	0.90±0.12*

*$P<0.05$ PS group vs control.

for 5 min. The specimens were examined under a fluorescence microscope (Olympus, C5060- ADU, Tokyo, Japan) and photographs were taken. The percentage of apoptotic rate was calculated by counting average TUNEL positive cells in three microscopy fields (positive cells / total cells).

Cell cycle analysis

After PS treatment, ascites were extracted (as describe in section 2.4) from each mouse at 0, 1, 3 and 5 d and washed with ice-cold PBS for three times. Cells were suspended in PBS and adjusted to a concentration of 2×10^6/mL, then fixed in 70% methanol. DNA was stained with propidium iodide (50 μg/mL) containing 5 mg/ml RNase (Boehringer Mannheim, Germany) at a 1:100 dilution. Cell cycle analysis was performed with a FACScan flow cytometer (Becton Dickinson, San Jose, CA, USA). The sub-G1/G0 cell fraction was considered as representative of apoptotic cells.

Immunofluorescence assay

Fresh ascetic fluid extracted from mice treated with PS for 0, 1, 3 and 5 d was washed three times with PBS (as describe in section 2.4). Cells were fixed with 4% paraformaldehyde for 25 min and permeabilized with 0.1% Triton X-100 for 5 min at room temperature. Next, slides were incubated with 0.1% BSA in PBS at room temperature for 30 min to block nonspecific antibody binding. Subsequently, slides were incubated with primary antibodies of Mouse Anti-Cyclin D1, Mouse Anti-P21, Rabbit Anti-Fas, Rabbit Anti-BCL-2, Mouse Anti-BAX, Mouse Anti-AFP and Rabbit Anti-caspase-3 (1:200 in 0.1% BSA, Santa Cruz Biotechnology, Santa Cruz, CA, USA). After overnight incubation at 4°C, the slides were washed and incubated with FITC-conjugated goat anti-mouse or goat anti-rabbit secondary antibody (1:200 in BSA, Beijing Jinqiao Biological Technology, Beijing, China) at 37°C in the dark for 1.5 h. Slides were washed with PBS and examined using a fluorescence microscope to count the positive cells (Olympus). The primary antibody was replaced with PBS in the negative control.

Statistical analysis

Experiments were performed at least 3 times, obtaining similar results. Results were expressed as mean ± SD, and differences between groups were assessed by *t* test using SPSS software. $P < 0.05$ was considered statistically significant.

Results

Effect of PS on life span and organ index

PS significantly affected mice survival time with longer life span, which indicated that PS inhibited the development of H22 tumor cell on mice as shown in

Tab.1. A significant difference ($P<0.05$) was found between control group and PS treated group on thymus index, but not on spleen index.

Morphological changes analyzed by HE staining

HE staining showed regular rounded shape cells with a big nucleus and dark color in control group as shown in Fig.1a. After PS treatment, the typical apoptotic morphology appeared such as cell shrinkage, cytoplasm and chromatin condensation and the formation of apoptotic bodies and cell debris after cell necrosis (Fig.1 b-d). The present cytomorphology results suggested that apoptosis might occur after PS treatment in H22 cells.

Induction of apoptosis by PS

TUNEL staining was performed to determine whether, in addition to the effects on cell morphology with the appearance of the typical apoptotic bodies, PS was also able to induce the break of DNA double helix in fragments at a molecular level. As shown in Fig.2, cells with green fluorescence increased in number as a result of the extension of the PS incubation time. The apoptotic rate increased from 38.85%±3.44% in the control group to 51.36%±1.50% in the experimental group treated with 1500mg/kg PS for 5 d ($P<0.05$). The present data were in accordance with the results obtained in the cell cycle analysis, which demonstrated that PS prevented cell survival and induced apoptosis in H22 cells according to the preserved DNA content and DNA broken chain.

Effect of PS on cell cycle distribution

H22 cell suspension was fixed with ice-cold 70% methanol and stained with PI for cell cycle and apoptosis analysis by flow cytometry (FCM). As shown in Fig.3,
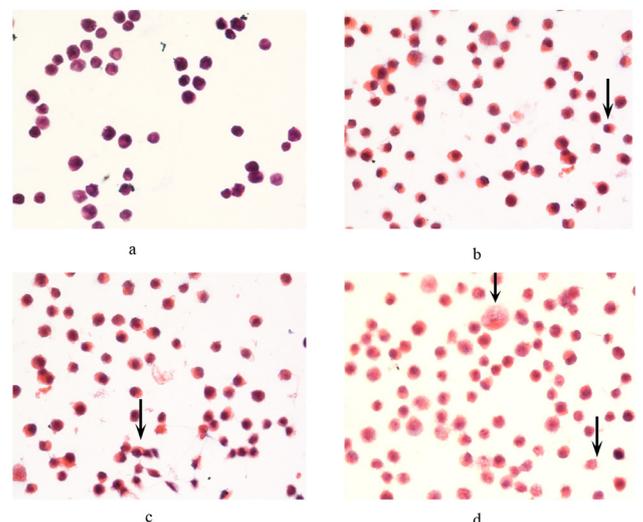

Figure 1. Morphological changes of H22 cell induced by PS (400×). (a) Control (0 d); (b) 1 d treatment; (c) 3 d treatment; (d) 5 d treatment.
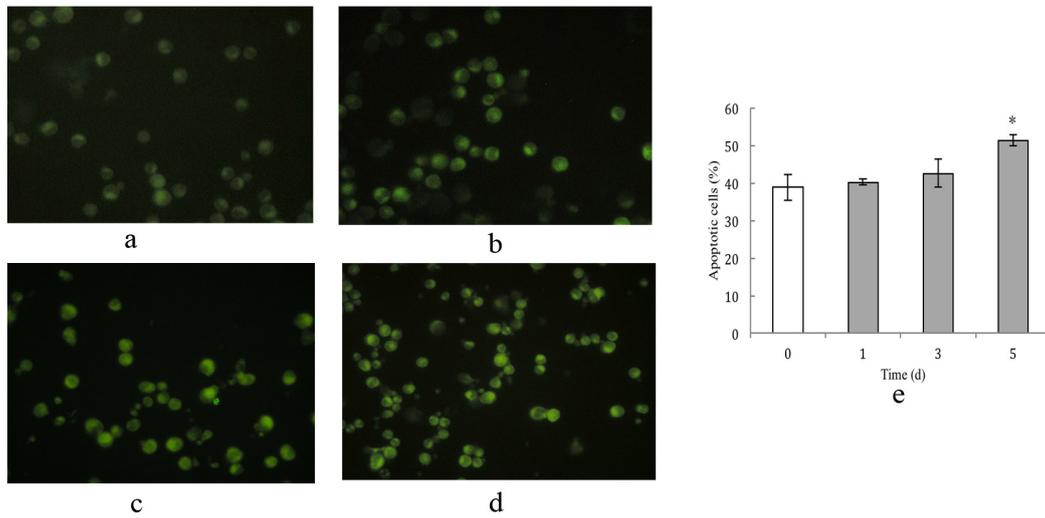
Figure 2. Effect of PS on H22 apoptosis analyzed by TUNEL assay. Mice were divided into five groups including control (PBS), 1, 3, 5d treated group (ascetic fluids and PS)and vehicle control (ascetic fluids and normal saline). In each group there were 15 mice. Ascites tumor cells were extracted, prepared and cytospun on slides with concentration of 1×10^6 cells/ ml for measurement of TUNEL staining using fluorescence microscopy ($400\times$). (a) Control (0 d); (b) 1 d treatment; (c) 3 d treatment; (d) 5 d treatment; (e) Apoptotic rate of H22 cells in ascites treated with PS. *$P<0.05$ vs control.
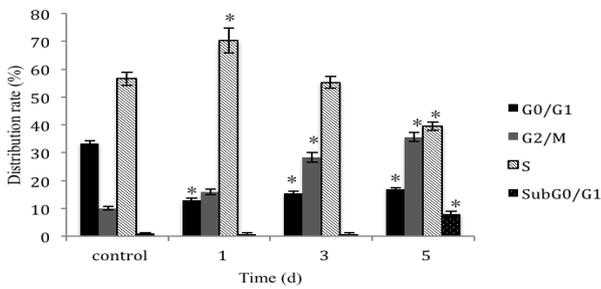

Figure 3. Apoptosis and cell cycle distribution of H22 cell. Ascitic KM mice were treated with PS for 1, 3 or 5 days with 15 mice in each group. Ascites tumor cells were extracted and prepared for cell cycle analysis by flow cytometry. Untreated cells (0 d) were used as control. *$P<0.05$ between each treated group and control group (0 d).

G_0/G_1 phase population was significantly decreased in PS treated cells compared with the control group, whereas the percentage of G_2/M increased as a result of the increased PS incubation time. Cell population of Sub-G_0/G_1 significantly increased ($P<0.05$) at 5 days after PS treatment, indicating a remarkable apoptosis induced by PS with G_2/M arrest.

Expression of apoptotic relevant proteins

To further confirm the effect of PS on H22 cell cycle arrest, we analyzed the expression of cyclin D1 and p21 proteins by immunofluorescent staining. On one hand, Cyclin D1 expression was remarkably down regulated from 60.89%±4.86% in control group to 48.75%±2.15% and 43.46%±2.46% in the 3 d and 5 d PS treatment, respectively, as shown in Fig.4 a, b, e. On the other hand, P21 protein expression was significantly upregulated from 30.25%±2.21% in control group to 68.55%±3.54% and 72.89%±1.87% in the 3 d and 5 d PS treatment, respectively, as shown in Fig.4 c, d and e. The similar trend was observed in western blotting results as showed in Fig.6. These results suggest that inactivation of Cyclin-D1 and P21 in H22 cells may play an important role in the course of PS-induced apoptosis.

A small and not statistically significant decrease of Fas protein was found at 1 d after PS treatment compared with the control group. However Fas significantly increased ($P<0.05$) to 45.39%±2.25% and 69.76%±3.50% in the 3 and 5 d PS treatment, respectively. Western blotting analyses were performed to address the roles of the Fas signaling pathways in the process of apoptosis induced by PS. The bands showed that
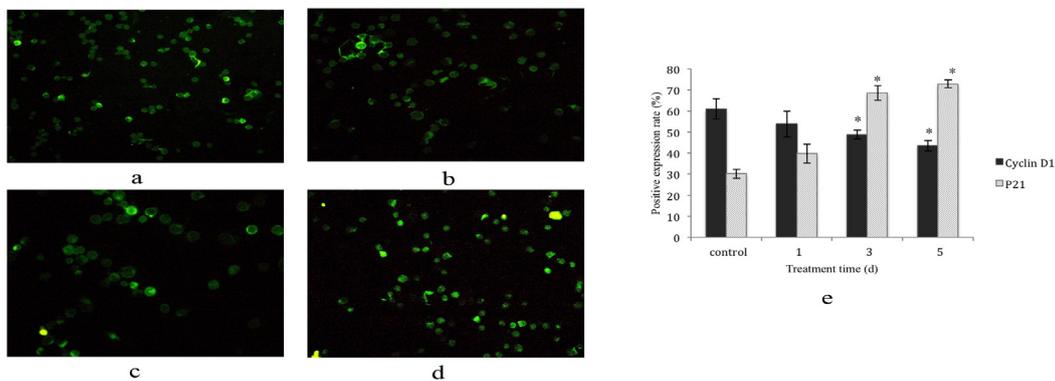

Figure 4. Expression of Cyclin D1 & P21 protein of H22 cells detected by immunohistochemistry ($400\times$). KM mice were treated with PS for 1, 3 or 5 days with 15 mice in each group. Ascites tumor cells were extracted and prepared for immunohistochemistry of Cyclin D1 and P21. (a) Expression of Cyclin D1 in control group (0 d); (b) Expression of Cyclin D1 in the treatment group (1500mg/g, 5 d treatment); (c) Expression of P21 in control group (0 d); (d) Expression of P21 in the treatment group (1500mg/g, 5 d treatment); (e) expression of Cyclin D1 and P21 protein of H22 cells. *$P<0.05$ between each treated group and control group.
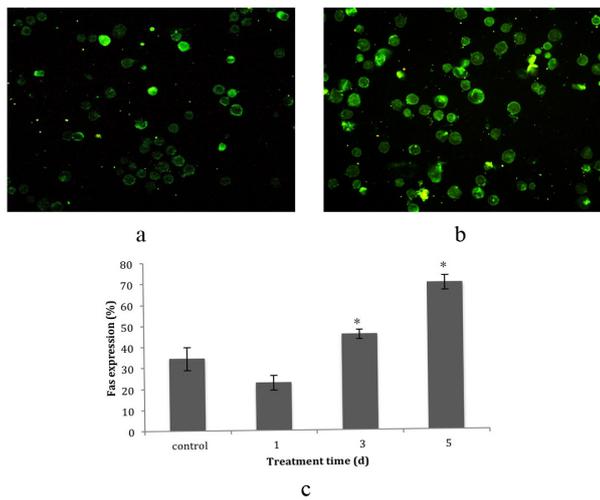
a

b

c

Figure 5. The effect of PS on the expression of Fas protein on H22 cells detected by immunohistochemistry (200×). KM mice were treated with PS for 1, 3 or 5 days with 15 mice in each group. Ascites tumor cells were extracted and prepared for immunohistochemistry of Fas expression. (a) Expression of Fas in control group (0 d); (b) expression of Fas in treatment group (1500mg/g, 5 d); (c) expression of Fas on H22 cells. *$P<0.05$ between each treated group and control group (0 d).
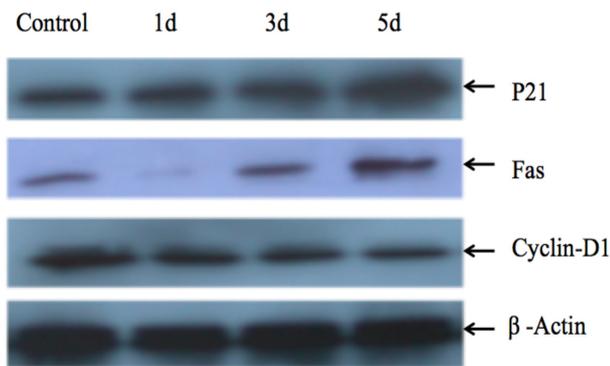

Figure 6. Function of P21, Fas and Cyclin-D1 in apoptosis induced by PS. Ascitic KM mice were treated with PS for 1, 3 or 5 days. Time course analysis of P21, Fas and Cyclin-D1 activation was assessed by western blot analysis. Untreated cells (0 d) were used as control.

Fas decreased after 1d treatment, however increased for 3 and 5d (Fig.6). Fas, as a transmembrane receptor protein, possesses a death domain to start cell apoptosis. BCL2 and BCL-xL are involved in type 2 Fas apoptosis pathway. In the present study, as shown in Fig.7 and Tab.2, BCL2 expression was significantly down regulated from 69.39%±5.02% in the control group to 52.60%±5.13% in the PS treated group right after 1 d treatment. This decrease remarkably proceeded until reaching 40.10%±2.89% and 34.56%±2.01% in the 3 and 5 d treatment, respectively ($P<0.05$). On the other hand, the expression of BAX expression was significantly increased after PS treatment from 19.64%±4.14%
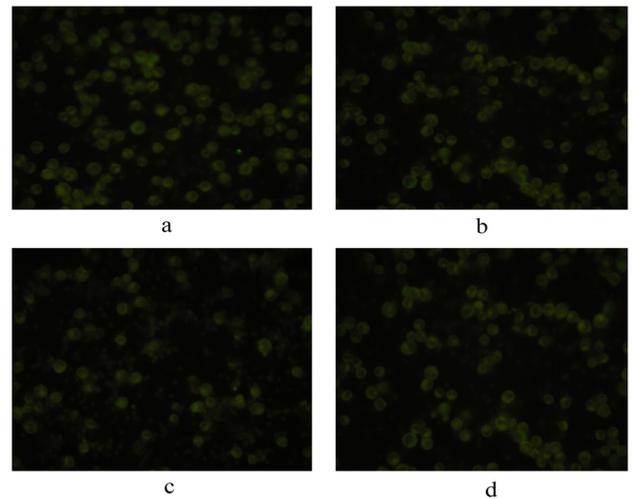

a

b

c

d

Figure 7. Expression of BCL-2 & Bax protein of H22 cells detected by immunohistochemistry (400×). KM mice were treated with PS for 1, 3 or 5 days with 15 mice in each group. Ascites tumor cells were extracted and prepared for immunohistochemistry of BCL-2 and Bax expression. (a) Expression of BCL-2 in control group (0 d); (b) Expression of BCL-2 in the treatment group (1500mg/g, 5 d treatment); (c) Expression of Bax in control group (0 d); (d) Expression of Bax in the treatment group (1500mg/g, 5 d treatment).

to 37.91%±3.10%, 50.43%±2.14% and 56.47%±3.27% in the 1, 3 and 5 d treatment groups, respectively. Taken together, these results demonstrate that modulation of BCL2 and BAX in H22 may play an important role in PS-induced apoptosis. The apoptotic process is mostly mediated by the caspase family proteins, since they are a set of proteases involved in the early apoptosis and on the delivery of the signaling pathway. Therefore, we investigated the contribution of caspase-3 on PS-induced apoptosis by immunofluorescent staining. A remarkable increase in the caspase-3 protein level was observed in H22 cells at day 1, 3 and 5 (Fig. 8), suggesting an important role for this signaling pathway in PS-induced apoptosis. Alpha-fetoprotein (AFP) has been considered as one of the major marker for liver cancer identification, which is detected in the cytoplasm by immunofluorescence method. Tab.3 showed that after 3 d of PS treatment, AFP expression was significantly down regulated from 55.12%±2.44% to 26.26%±0.67%, and this amount remained low over time to day 5. Hence, the extension of the survival time and the increase in life span may be due to the AFP down regulation by PS treatment.

Discussion

It is already known the ability of PS to inhibit the growth of MCF-7 breast cancer cells and K562 leukemia cells as well as its ability to induce cell apoptosis, as we showed in our previous study (27-29). Based on

Table 2. Expression of BCL-2 and Bax protein of H22 cells.

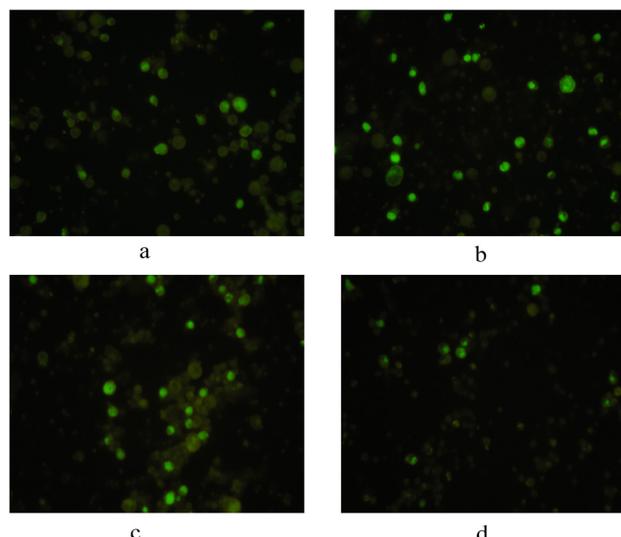| Treatment time (d)	BCL-2 expression (%)	Bax expression (%)	BCL-2/Bax
0	69.39±5.02	19.64±4.14	3.53
1	52.60±5.13*	37.91±3.10*	1.38
3	40.10±2.89*	50.43±2.14*	0.79
5	34.56±2.01*	56.47±3.27*	0.61

*$P<0.05$ between each treated group and control group.

Figure 8. Expression of Caspase-3 & AFP protein of H22 cells detected by immunohistochemistry (400×). KM mice were treated with PS for 1, 3 or 5 days with 15 mice in each group. Immunohistochemistry were performed for Caspase-3 and AFP expression of Ascites tumor cells. (a) Expression of Caspase-3 in control group (0 d); (b) Expression of Caspase-3 in the treatment group (1500mg/g, 5 d treatment); (c) Expression of AFP in control group (0 d); (d) Expression of AFP in the treatment group (1500mg/g, 5 d treatment).

Table 3. Expression of Caspase-3 and AFP protein of H22 cells.

Treatment time (d)	Caspase-3 (%)	AFP expression (%)
0	23.07 ± 0.68	55.12 ± 2.44
1	$35.50 \pm 1.26^*$	50.89 ± 1.77
3	$43.41 \pm 3.83^*$	$26.26 \pm 0.67^*$
5	$75.62 \pm 4.72^*$	$22.04 \pm 1.84^*$

$*P < 0.05$ between each treated group and control group.

our preliminary study, H22 mice ascitic tumor model was chosen to evaluate the antitumor activity of PS. We showed that PS prolonged survival time of the mice, so as to increase the life span (Tab. 1). However PS didn't show significant effect on spleen index and even reversely effected the thymus index, which indicated that PS improve mice survival condition not through enhancing immunologic function. Therefore we speculated that PS might inhibit cell proliferation by inducing cell apoptosis. After morphology observation, typical apoptotic characteristics were appeared (Fig. 1), besides, DNA fragmentations have been detected by TUNEL assay (Fig. 2), On the basis of our results, tumor cell proliferation might be inhibited by PS through the induction of H22 cell apoptosis.

The cell cycle is regulating a set of cellular signaling systems that not only control cell proliferation, but also determine the subsequent fate of the daughter cells by controlling the processes of differentiation, apoptosis or senescence (30-32). Cell cycle blockage is the main target for many anticancer drugs, such as Adriamycin, Cis-platinum, 5-fluorouracil and Taxoids. Some studies indicated that cell cycle arrest on G_2/M or S phase depends on the cell sensitivity to cancer (33, 34). In the present study, cell cycle arrest on G_2/M phase was observed after 1 and 3 d of PS treatment, decreasing the number of cells that moved from G_2/M to G_1 phase. Cell cycle signaling is responsible for controlling the survival of a cell, including the detection and repair of genetic damage as well as the prevention of cell division

(35). Two key categories of regulatory molecules of the signaling system, cyclins and cyclin-dependent kinases (CDKs), control the cell cycle progress mediated by the bind to specific CDKs to form cyclin/CDK complexes. In our results, the up-regulation of P21, a potent cyclin dependent kinase inhibitor (CKI), that bind and inhibit cyclin-CDKs complexes activity, prevented the DNA damaged cell to move from G_1 to S phase, thus inhibiting cell proliferation. On the other hand, cyclin D1, as one of the main cyclins regulating the proliferation that plays an important role in the G_1 to S transition, was significantly down regulated at 3 and 5 d after PS treatment, indicating that also this protein was involved in the reduced cell proliferation. Furthermore, AFP down regulation was detected at 3 d after PS treatment. Since it is also known that AFP inhibits cell proliferation by inducing a delay in the progression from the G_1 to S phase, decrease of cells in G0/G1phase and a G2/M arrest might due to the down-regulation of Cyclin D1 and AFP and up-regulation of P21 proteins.

Two typical caspase-dependent apoptotic pathways are involved in the apoptosis of the cell, one involving the death receptor pathway and the other one the mitochondrial pathway (36). Death receptors, like Fas, TRAIL receptors and TNF receptor, can activate caspase-8 and -10 to initiate the caspase cascade (37). In our results the expression of Fas significantly increased after PS treatment. As a consequence of that, it is known that the permeability of the mitochondria outer membrane is changed and releases the cytochrome C to finally activate caspase-9. Once activated, a cascade of caspases are gradually and subsequently involved in a chain reaction where each caspase are cleaved and activated until the activation of caspase-3 that represent the final step leading to apoptosis. In our results, caspase-3 remarkably increased at 1, 3 and 5 d after PS treatment. Following Fas activation in H22 cells, a balance between the anti-apoptotic protein BCL2 and the pro-apoptotic protein of BAX is established, which work together to control the cell fate. Our immunofluorescence assay results showed a down regulation of BCL2 expression and an up regulation of BAX expression, leading to an activation of the caspase-activated Fas pathway in PS-induced H22 apoptosis.

In conclusion, the present study showed that PS-induced ascitic tumor H22 apoptosis is possibly mediated by cell population decrease in G_0/G_1 phase and G_2M arrest and furthermore by BCL2/BAX involved in caspase-activated Fas pathway. Our results provide new insights into the possible molecular mechanism of PS as a novel anticancer agent and its potential use in clinic.

References

1. Chen, J. G.; Zhang, S. W. In Liver cancer epidemic in China: past, present and future, *Semin. Cancer. Biol.* 2011, **21**: 59-69.

doi:10.1016/j.semcancer.2010.11.002

2. Cairns, R. A.; Harris, I. S.; Mak, T. W., Regulation of cancer cell metabolism. *Nat. Rev. Cancer.* 2011, **11**: 85-95. doi:10.1016/j.semcancer.2010.11.002

3. Li, W.; Rao, D. K.; Kaur, P., Dual role of the metalloprotease FtsH in biogenesis of the DrrAB drug transporter. *J. Biol. Chem.* 2013, **288**: 11854-64. doi: 10.1074/jbc.M112.441915

4. Mohankumar, K.; Pajaniradje, S.; Sridharan, S.; Singh, V. K.; Ronsard, L.; Banerjea, A. C.; Benson, C. S.; Coumar, M. S.; Rajagopalan, R., Mechanism of apoptotic induction in human breast cancer cell, MCF-7, by an analog of curcumin in comparison with curcumin–An in vitro and in silico approach. *Chem-bio. Interact.* 2014, **210**: 51-63. doi: 10.1074/jbc.M112.441915

5. Kerr, J. F.; Wyllie, A. H.; Currie, A. R., Apoptosis: a basic biological phenomenon with wide-ranging implications in tissue kinetics. *Brit. J. Cancer.* 1972, **26**: 239. doi:10.1038/bjc.1972.33

6. Wyllie, A. H.; Kerr, J. R.; Currie, A., Cell death: the significance of apoptosis. *Int. Rev. Cytol.* 1980, **68**: 251-306. doi:10.1016/S0074-7696(08)62312-8

7. Strasser, A.; O'Connor, L.; Dixit, V. M., Apoptosis signaling. *Ann. Rev. of Biochem.* 2000, **69**: 217-245. doi: 10.1146/annurev.biochem.69.1.217

8. Okada, H.; Mak, T. W., Pathways of apoptotic and non-apoptotic death in tumour cells. *Nat. Rev. Cancer*. 2004, **4**: 592-603. doi: 10.1146/annurev.biochem.69.1.217

9. Cullen, S. P.; Martin, S. J. In Fas and TRAIL 'death receptors' as initiators of inflammation: Implications for cancer. *Semin. Cell Dev. Biol.* 2015, **39**: 26-34. doi:10.1016/j.semcdb.2015.01.012

10. Hyman, B. T.; Yuan, J., Apoptotic and non-apoptotic roles of caspases in neuronal physiology and pathophysiology. *Nat. Rev. Neurosci.* 2012, **13**: 395-406. doi:10.1016/j.semcdb.2015.01.012

11. White, M. J.; McArthur, K.; Metcalf, D.; Lane, R. M.; Cambier, J. C.; Herold, M. J.; van Delft, M. F.; Bedoui, S.; Lessene, G.; Ritchie, M. E., Apoptotic Caspases Suppress mtDNA-Induced STING-Mediated Type I IFN Production. *Cell.* 2014, **159**: 1549-1562. doi:10.1016/j.cell.2014.11.036

12. Ola, M. S.; Nawaz, M.; Ahsan, H., Role of Bcl-2 family proteins and caspases in the regulation of apoptosis. *Mol. Cell. Biochem.* 2011, **351**: 41-58. doi:10.1007/s11010-010-0709-x

13. Rincheval, V.; Bergeaud, M.; Mathieu, L.; Leroy, J.; Guillaume, A.; Mignotte, B.; Le Floch, N.; Vayssière, J.-L., Differential effects of Bcl-2 and caspases on mitochondrial permeabilization during endogenous or exogenous reactive oxygen species-induced cell death. *Cell Biol. Toxicl.* 2012, **28**: 239-253. doi:10.1007/s11010-010-0709-x

14. Salvesen, G. S., Caspases: opening the boxes and interpreting the arrows. *Cell. Death. Differ.* 2002, **9**: 3-5. doi: 10.1038/sj.cdd.4400963

15. Ghavami, S.; Hashemi, M.; Ande, S. R.; Yeganeh, B.; Xiao, W.; Eshraghi, M.; Bus, C. J.; Kadkhoda, K.; Wiechec, E.; Halayko, A. J., Apoptosis and cancer: mutations within caspase genes. *J. Med. Genet.* 2009, **46**: 497-510. doi: 10.1038/sj.cdd.4400963

16. Shamas-Din, A.; Kale, J.; Leber, B.; Andrews, D. W., Mechanisms of action of Bcl-2 family proteins. *Cold. Spring. Harb. Perspect. Biol.* 2013, **5**: a008714. doi: 10.1101/cshperspect.a008714

17. Harper, J.; Adams, P., Cyclin-dependent kinases. *Chem. Rev.* 2001, **101**: 2511-2526. doi: 10.1101/cshperspect.a008714

18. Andreu, Z.; Khan, M. A.; González Gómez, P.; Negueruela, S.; Hortigüela, R.; San Emeterio, J.; Ferrón, S. R.; Martínez, G.; Vidal, A.; Fariñas, I., The Cyclin Dependent Kinase Inhibitor p27kip1 Regulates Radial Stem Cell Quiescence and Neurogenesis in the Adult Hippocampus. *Stem. Cells.* 2015, **33**: 219-229. doi:10.1002/stem.1832

19. Baldin, V.; Lukas, J.; Marcote, M.; Pagano, M.; Draetta, G., Cyclin D1 is a nuclear protein required for cell cycle progression in G1. *Gen. Dev.* 1993, **7**: 812-821. doi:10.1101/gad.7.5.812

20. Lim, S.; Kaldis, P., Cdks, cyclins and CKIs: roles beyond cell cycle regulation. *Development*. 2013, **140**: 3079-3093. doi:10.1242/dev.091744

21. Pope, P. A.; Bhaduri, S.; Pryciak, P. M., Regulation of cyclin-substrate docking by a G1 arrest signaling pathway and the Cdk inhibitor Far1. *Curr. Biol.* 2014, **24**: 1390-1396. doi:10.1242/dev.091744

22. Liao, W.; Ning, Z.; Ma, L.; Yin, X.; Wei, Q.; Yuan, E.; Yang, J.; Ren, J., Recrystallization of dihydromyricetin from Ampelopsis grossedentata and its anti-oxidant activity evaluation. *Rejuv. Res.* 2014, **17**: 422-9. doi: 10.1021/jf504677r

23. Ren, L.; Perera, C.; Hemar, Y., Antitumor activity of mushroom polysaccharides: a review. *Food & Funct..* 2012, **3**: 1118-1130. doi:10.1039/C2FO10279J

24. Fan, L.; Ding, S.; Ai, L.; Deng, K., Antitumor and immuno-modulatory activity of water-soluble polysaccharide from Inonotus obliquus. *Carbohyd. Polym.* 2012, **90**: 870-874. doi:10.1016/j.carbpol.2012.06.013

25. Liao, W.; Luo, Z.; Liu, D.; Ning, Z.; Yang, J.; Ren, J., Structure characterization of a novel polysaccharide from Dictyophora indusiata and its macrophage immunomodulatory activities. *J. Agr. Food. Chem.* 2015, **63**: 535-44. doi: 10.1021/acs.jafc.5b00614

26. Patra, D.; Sandell, L. J., Antiangiogenic and anticancer molecules in cartilage. *Expert. Rev. Mol. Med.* 2012, **14**:10. doi:10.1017/erm.2012.3

27. Song, W.; Jia, Y.; Fan, Y.; Du, M.; Liu, A., PDTC antagonized polysaccharide-induced apoptosis in MCF-7 cells through a caspase-8 mediated Fas pathway. *J. Funct. Foods.* 2013, **5**: 1270-1278. doi: 10.1016/j.jff.2013.04.011

28. Song, W.; Hu, P.; Shan, Y.; Du, M.; Liu, A.; Ye, R., Cartilage polysaccharide induces apoptosis in K562 cells through a reactive oxygen species-mediated caspase pathway. *Food. & Funct.* 2014, **5**: 2486-2493. doi:10.1039/C4FO00476K

29. Liu, A. J.; Song, W.; Yang, N.; Liu, Y. J.; Zhang, G. R., Cartilage polysaccharide induces apoptosis in human leukemia K562 cells. *Cell. Biol. Toxicol.* 2007, **23**: 465-76. doi:10.1007/s10565-007-9008-z

30. Cheung, T. H.; Rando, T. A., Molecular regulation of stem cell quiescence. *Mol. Cell. Biol.* 2013, **14**: 329-340. doi:10.1038/nrm3591

31. Yang, G.; Li, W.; Liao, W.; Zhang, X.; Zou, Y.; Dai, J.; Li, Y.; Jing, C.; Zhou, T., Identification of the Alternative Splicing of the UL49 Locus of Human Cytomegalovirus. *BioMed Res. Int.* 2015, **2015**: 280-276. doi.:10.1155/2015/280276

32. Li, W.; Sharma, M.; Kaur, P., The DrrAB Efflux System of Streptomyces peucetius Is a Multidrug Transporter of Broad Substrate Specificity. *J. Biol. Chem.* 2014, **289**: 12633-12646. doi: 10.1074/jbc.M113.536136

33. Vijayaraghavalu, S.; Dermawan, J. K.; Cheriyath, V.; Labhasetwar, V., Highly synergistic effect of sequential treatment with epigenetic and anticancer drugs to overcome drug resistance in breast cancer cells is mediated via activation of p21 gene expression leading to G2/M cycle arrest. *Mol. Pharmaceutics.* 2013, **10**: 337-352. doi: 10.1021/mp3004622

34. Hseu, Y.-C.; Lee, M.-S.; Wu, C.-R.; Cho, H.-J.; Lin, K.-Y.; Lai, G.-H.; Wang, S.-Y.; Kuo, Y.-H.; Senthil Kumar, K.; Yang, H.-L., The chalcone flavokawain B induces G2/M cell-cycle arrest and apoptosis in human oral carcinoma HSC-3 cells through the intracellular ROS generation and downregulation of the Akt/p38 MAPK signaling pathway. *J.Agr. Food. Chem.* 2012, **60**: 2385-2397. doi: 10.1021/jf205053r

35. Blanpain, C.; Mohrin, M.; Sotiropoulou, P. A.; Passegue, E.,

DNA-damage response in tissue-specific and cancer stem cells. *Cell Stem Cell* 2011, **8**: 16-29. doi:10.1016/j.stem.2010.12.012

36. Nakajima, E.; Hammond, K.; Shearer, T.; Azuma, M., Activation of the mitochondrial caspase pathway and subsequent calpain activation in monkey RPE cells cultured under zinc depletion. *Eye.* 2014, **28**: 85-92. doi:10.1038/eye.2013.239

37. Mocarski, E. S.; Upton, J. W.; Kaiser, W. J., Viral infection and the evolution of caspase 8-regulated apoptotic and necrotic death pathways. *Immunology.* 2012, **12**: 79-88. doi:10.1038/nri3131